International Journal of Environmental Science and Technology
https://doi.org/10.1007/s13762-024-05989-8

ORIGINAL PAPER

Performance evaluation of microbial fuel cells for bioelectricity generation: influence of potential scan-rate and real-time external load

I. Meshack Simeon[1,2] · A. Gbabo[1] · R. Freitag[2]

Received: 19 January 2024 / Revised: 17 June 2024 / Accepted: 14 August 2024

Abstract
The electrochemical performance of microbial fuel cells is conventionally assessed through linear sweep voltammetry at predefined potential scan rates. Nevertheless, this approach frequently falls short in representing the long-term behavior of microbial fuel cells under actual external loads, highlighting the need for a standardized evaluation method incorporating both linear sweep voltammetry and external loads. To address this gap, this study evaluates the performance of single-chamber microbial fuel cells under different loads and scan rates. The MFCs were tested with external loads of 1200, 470, and 270 Ω, derived from maximum power points of polarization sweeps at scan rates of 0.1, 0.5, and 1 mV/s at two operational phases. Power estimates at these scan rates were 61.96, 87.88, and 166.68 mW/m^2 at current densities of 116.5, 229.6, and 403 mA/m^2, respectively. In the initial two hours, average power densities with 1200, 470, and 270 Ω were 73 ± 16.7, 36.3 ± 42, and 88.5 ± 120.1 mW/m^2, respectively. Over the long term, the fuel cells under constant loading with resistance estimated at 0.1 mV/s showed average power 73.7% and 89.1% higher than those with resistances estimated at 0.5 mV/s and 1 mV/s, respectively, indicating that higher scan rates lead to overestimation of power. Although initially underestimated, the 0.1 mV/s scan rate more accurately reflected the true long-term performance of the fuel cells. This study emphasizes the importance of using appropriate scan rates for linear sweep voltammetry to obtain realistic long-term performance estimates of microbial fuel cells under real-time loads.

Keywords Bioelectricity · External load · Evaluation · Microbial fuel cell · Maximum power · Potential scan rate

Introduction

All nation's energy strategies now prioritize clean and renewable energy sources over conventional fossil fuels due to concerns about sustainability and environmental protection. Converting power plants to low-carbon and carbon-free fuels or using modern technologies to capture and store carbon is a crucial step towards decarbonizing the energy sector (Anika et al. 2022). Bio-electrochemical systems (BES) technology is a highly researched area in modern technology due to its adaptability and environmental friendliness. Microbial fuel cell (MFC) technology is a type of BES that utilizes the natural activities of electroactive bacteria or biofilm (EAB) to generate electricity while removing pollutants from their environment (Golzarian et al 2024). Basically, the EAB break down the organic content of their natural environment to release electrons through electrochemical redox reactions. Oxidation takes place at the anode when the microbes oxidize the substrate to generate electrons and protons (Pandit and Das 2017; Nawaz et al. 2020). This leads to the proliferation of bacterial cells and the accumulation of biofilm on the electrodes. When an external load is connected between the anode and cathode, a flow of electrons occurs, causing the cathode to take up electrons to reduce electron acceptors such as oxygen and nitrogen. MFCs are basically bioreactors that utilize

Editorial responsibility: M.Shabani.

✉ I. Meshack Simeon
s.imologie@futminna.edu.ng

[1] Department of Agricultural and Bioresources Engineering, School of Infrastructure, Process Engineering and Technology, Federal University of Technology, PMB 65, Minna, Nigeria

[2] Chair of Process Biotechnology, Faculty of Engineering Science, University of Bayreuth, Universitätsstraße 30 FAN-D, 2. Stock, 95447 Bayreuth, Germany

Published online: 09 September 2024

organic carbon waste (Simeon et al. 2019; Simeon and Raji 2016) and bacteria to convert chemical energy into electrical energy (Ameen et al. 2023). They are important devices that act as efficient carbon–neutral sources (Vinoth Kannan et al. 2023) for the recovery of bio-renewable resource (Miao et al. 2023) and waste treatment.

The performance of MFCs is usually based on different responses depending on the objective of the design, as MFCs are multipotent devices for wastewater treatment, bioremediation, resource recovery, etc. with simultaneous generation of bioelectricity. If the MFC is designed for wastewater treatment, the coulombic efficiency is often one of the most important parameters for evaluating MFC performance. Regardless of design, almost all MFCs generate electricity in addition to recovering other resources. Therefore, the electrical output of MFCs is typically based on the maximum power transfer (MPT) algorithm (Watson and Logan 2011). The maximum power point (MPP) is normally determined by linear sweep voltammetry (LSV) with a potentiostat at different potential sweeps or scan rates (PSR) (Zhao et al. 2009) or with variable resistors. The magnitude of the MPP parameters depends on the PSR when a potentiostat is used or on the time at which the so-called "pseudo-stability" is reached when variable resistors are used. This assessment of MFC performance using MPP parameters often does not reflect actual long-term performance under real-time external loads (Watson and Logan 2011), as the capacitive characteristics of most electrodes mean that the observed performance at a faster PSR is, in most cases, pure transients and does not reflect the actual long-term performance of the MFC.

The MPP of an MFC is the point, i.e., current and cell voltage on the power curve, at which the MFC delivers the maximum net power under polarization. The MPP parameters vary depending on several variables, such as the type and natural activities of the EAB, environmental conditions, system architecture, substrate availability (Aghababaie et al. 2015), PSR, external resistance, and time to reach pseudo-stability, etc. Therefore, the values of MPP parameters, which are often reported by different research groups and laboratories, are not uniform for similar system architectures. Furthermore, different researchers often report MFC performance at different PSR. For instance, Littfinski et al. reported comparable results for the performance of an air–cathode single-chamber MFC with LSV at PSR of 0.1 mV/s and varying circuit resistance for 15 min at each resistance (Littfinski et al. 2021). While most studies are conducted with PSR of 1 mV/s (Nam et al. 2018; Saadi et al. 2020; Simeon and Freitag 2022), PSR of 0.25 mV/s (Walter et al. 2019; Poli et al. 2020) have been reported. On the other hand, the time range between 5 and 30 min is most often reported (Kim et al. 2011; Peng et al. 2013; Walter et al. 2016; Wang et al. 2014) when performance evaluation is based on varying external resistance. These inconsistencies in the best time to achieve pseudo-stability with real-time external loads (RTEL) and the best PSR for obtaining the MPP of MFCs complicates universal standardization of their performance. It is therefore important to use a reliable and consistent method for evaluating the electrical performance of MFCs to obtain valid MPP results which can be compared with performance of different or similar MFC studies under the same or different conditions. In addition, selecting the appropriate RTEL has been a significant bottleneck in evaluating MFCs. Many studies report performance metrics based on arbitrarily chosen RTEL values (Wang et al. 2014; Walter et al. 2019; Golzarian et al 2024) while others limit their evaluations to the electrochemical performance using LSV (Saadi et al. 2020; Simeon and Freitag 2022; Littfinski et al. 2021). In the latter case, proper enrichment of the MFCs with the EAB may not occur, especially if the MFCs under study are only operated under open circuit conditions. MFCs exhibit varying performance behaviors and electrochemical responses (Lepage et al. 2014) influenced by several factors, including the activity of constituent microbes, types of substrates, electrode materials, external load, and environmental conditions. Connecting the appropriate resistor at each phase of operation can facilitate the enrichment of MFCs with the optimal electroactive microbes (Li et al. 2024) and enhance their long-term performance.

Among the variables that influence MFC performance, PSR and RTEL are the most important parameters if the evaluation of the MFC is based on extracting the maximum power. Realizing the full potential of MFCs should be the primary emphasis of their development and evaluation, since they are part of BES that are crucial to the energy transition and environmental protection. To determine the relevance of the MPP in terms of applicability when evaluating the actual power of the MFC, the following questions are pertinent: Is it possible to obtain a maximum power comparable to the maximum power determined from the LSV if the resistance determined from the MPP is connected externally to the MFC? If so, can the power be maintained over a long operating period? At which PSR can the MPP parameters predict the external load for sustainable maximum power from the MFC? To date, no study has been conducted to address these issues and determine the relationship between PSR and RTEL in maximizing the actual electrical performance of the MFC.

To address these questions, single-chamber soil MFCs were assembled in which soil mixed with water to form mud served as a nutrient-rich electrolyte, a source of electroactive bacteria, and a means for exchange of protons. The short-term and long-term performance of the MFCs were evaluated with RTEL determined from the MPP based on different PSRs during different stages of polarization of the MFCs. The objective was to identify the optimal PSR for

determining the external resistance that enables sustainable maximum power extraction from the MFC, thereby providing a more accurate assessment of the long-term performance of the soil MFC.

Materials and methods

MFCs assembly and operation

Six (6) Single-chamber MFCs were set up in which biologically active soil mixed with water to form mud served as a nutrient-rich electrolyte, a source of electroactive bacteria, and a medium for the exchange of protons and cations. The anode and cathode were made of a modified stainless-steel mesh coated with a conductive paste made of vulca-72 and epoxy binder. The fabrication of the electrode was carried out by the method of pasting and reinforcement described previously (Simeon et al. 2022a, 2021). The MFCs were assembled by placing about 1 cm layer of mud at the base of the cells before installing the anode. 3 cm (approximately, 230 g) layer of mud was added above the anode before installing the cathode which was exposed to the overlying air above the cells. A detailed description of the assembly of the MFCs has been previously reported (Simeon and Freitag 2022).

The Six MFCs were divided into two groups for investigating the effect of LSV and determining the resistance at MPP. Group 1 (3 MFCs): These MFCs were first operated under a constant external load of 470 Ω (Fig. S1a) after a stable open-circuit voltage (OCV) was reached. After maintaining this load for 120 h, the external load was disconnected. Data were then collected for an additional 180 h to allow the MFCs to stabilize under open-circuit conditions (Fig. S1 b) before performing LSV. This ensured minimal influence from the previous load on the LSV measurement. Group 2 (3 MFCs): These MFCs were operated without any additional external load beyond the data logger's input impedance (1 MΩ in single-ended mode) throughout the exponential growth phase.

Additionally, a separate MFC (control) was used to determine the optimal external resistance for maximum performance. LSV was not performed on this MFC. Instead, a series of external resistances ranging from 200 to 2000 Ω (chosen to be slightly different from the resistance calculated from the MPP of the LSV data of Group 1 and Group 2 MFCs) were applied sequentially to this MFC, starting from the highest value and decreasing incrementally. The constant load discharge function of EC-Lab (V11.32) was used for selecting the actual load. After each discharge cycle, the MFC was allowed to rest for at least 24 h under open-circuit conditions (with only the data logger connected) to regain stability before applying the next load or resistance. This control experiment allowed for the identification of the RTEL that yielded the best performance without the influence of LSV pre-treatment. The MFCs were connected to a multi-channel data logger (ADC-24, input impedance for single ended: 1MΩ, differential: 2MΩ) for continuous data capture before LSV experiments were conducted. The voltage of the MFCs was automatically recorded at an hour interval (unless otherwise stated) using the set-up proposed by Simeon (2023) (Fig. 1).

Determination of real time external loads at different potential scan rates (PSRs)

The Biologic Instrument (VMP3-France) was used to perform LSV at three (3) PSRs (0.1, 0.5 and 1 mV/s) during

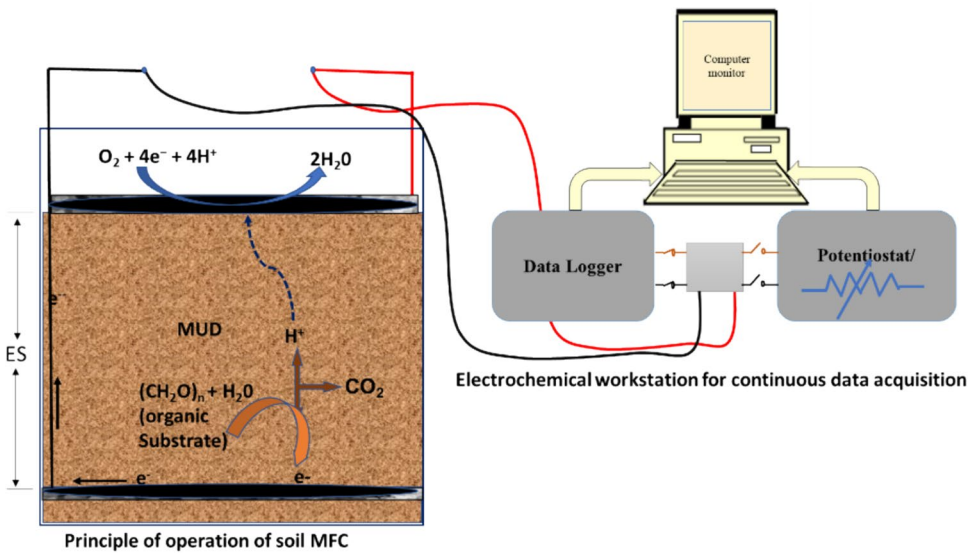

Fig. 1 A schematic description of MFC operation and electrochemical workstation for performance evaluation

two phases of the MFCs operation: 1) during the steady maximum OCV of three of the MFCs and 2) during the exponential growth in OCV of the remaining three MFCs. Polarization and power curves were produced from the LSV data from which the MPP parameters were determined as illustrated in the power and polarization curves (Fig. 2).

For symmetrical curves around the center, the optimum resistance for maximum power (R_{mpp}) was taken to be approximately equal to the total internal resistance ($\mathbf{R_{int}}$) determined from Eq. 1 otherwise, R_{mpp} was estimated from Eq. 5.

$$R_{\mathrm{mpp}} = R_{\mathrm{int}} = \frac{V_{\mathrm{mpp}}}{I_{\mathrm{mpp}}} \tag{1}$$

The measured cell voltage (E_{cell}) for MFCs is usually a linear function of the current and can be simplified as described with Eq. 2 (Logan et al. 2006).

$$E_{\mathrm{cell}} = E_{\mathrm{oc}} - IR_{\mathrm{int}} \text{ or } E_{\mathrm{oc}} = E_{\mathrm{cell}} + IR_{\mathrm{int}} = IR_{ext} + IR_{\mathrm{int}} \tag{2}$$

By converting Eq. 2, the internal resistance can be calculated as

$$\mathbf{R_{int}} = \frac{E_{oc} - \mathbf{E_{cell}}}{\mathbf{I}} \tag{3}$$

The generated current (**I**) can be described by Ohm's law given in Eq. 4

$$\mathbf{I} = \frac{\mathbf{E_{cell}}}{\mathbf{R_{ext}}} \tag{4}$$

By applying Eq. 4 in Eq. 3, the internal resistance is

$$\mathrm{R_{mpp}} = \left(\frac{\mathrm{E}_{oc}}{\mathrm{E_{cell}}} - 1\right) * \mathrm{R_{ext}} \tag{5}$$

where $\mathbf{R_{ext}}$ is the external resistance at which the maximum power was achieved during polarization. $E_{cell} = V_{mpp}$ = cell voltage at MPP. Besides MPP parameters, the short circuit current (I_s), theoretical maximum power ($\boldsymbol{P_T}$) and fill-factor (FF) were also obtained from the polarization and power curves as described in Table 1.

Results and discussion

Effect of PSR and RTEL on the MPP and long-term performance of the MFC

The effect of the PSR on the MPP was studied at two phases of the MFCs operation. The first evaluation was done at the steady-state performance when the voltage increased from

Table 1 Important parameters of the of the polarization and power curves

Symbol	Description	Applicable formula
$\mathbf{E_{oc}}$	Open-circuit potential or voltage	
MPP	Maximum power point	
P_{max}	Maximum power	$P_{max} = I_{max} * V_{max}$
V_{mpp}	Cell voltage at MPP	
I_{mpp}	Cell current at MPP	
I_S	Short-circuit current	
$\boldsymbol{P_T}$	Theoretical maximum power	$P_T = I_s * E_{oc}$
FF	Fill-factor	$FF = \frac{P_{max}}{P_T}$

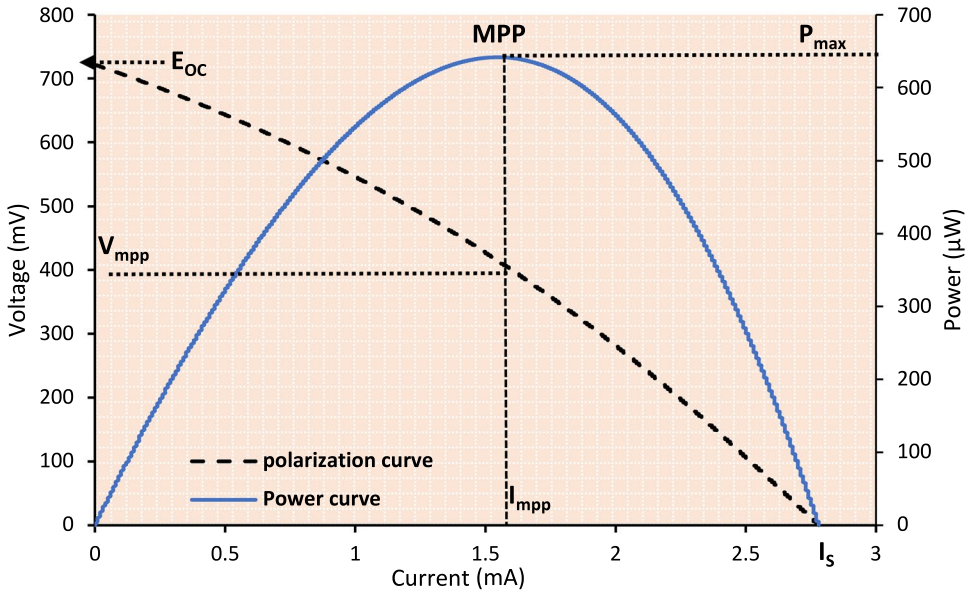

Fig. 2 Typical Polarization and power curves for the evaluation of MFCs performance

the lag phase to the maximum OCV. Secondly, another evaluation was carried out when the voltage of the MFCs was increasing at an exponential rate which is equivalent to the logarithmic phase of the bacteria growth cycle. Therefore, the discussion is based on these evaluation periods.

Effects of PSR and RTEL on the performance of MFCs in stationary phase

Figure 3a, b show the power density and polarization curves as a function of the current density and the power density curves as a function of the resistance during the LSV test. The power indices measured on the basis of the curves or calculated according to Table 1 are listed in Table 2.

There is a direct proportionality between the power and the PSR. The average OCV of the three MFCs at the point of polarization was 0.73 ± 0.1 V. Although the three MFCs did not attain the same value of OCV at the point of polarization (Fig. S1, their values were close with a standard deviation of only 0.1 V. Furthermore, a positive correlation between power output and PSR was observed. MFCs polarized at a PSR of 1 mV/s exhibited approximately 60% and 30% greater power output compared to those at 0.1 mV/s and 0.5 mV/s, respectively. In contrast, the lower the PSR, the higher the resistance as shown in Fig. 3b. R_1, $R_{0.5}$ and $R_{0.1}$ which are the resistance measured at PSR of 1, 0.5, 0.1 respectively, are presented as R_{mpp} in Table 2. The higher resistance at lower PSRs accounted for the lower MPPs. The implication is that power measured at different PSR are not equal unless there is some form of standardization. This difference in power at different PSR is usually more pronounced if the electrodes are made of materials with pseudocapacitive properties (Simeon et al 2021). This is similar to the report of Watson and Logan (2011) who reported that overestimation of the MFC performance may occur if LSV is used to evaluate the MFCs at PSR greater than 0.1 mV/s (Watson and Logan 2011).

Table 2 Performance indices at steady of the MFC at different PSRs

Parameters	$PSR_{0.1}$	$PSR_{0.5}$	PSR_1
Is (mA)	0.76	1.54	2.78
Eoc (mV)	858.00	603.00	721.00
PT (mW)	0.65	0.93	2.01
P_{max} (mW/m^2)	61.96	87.88	166.68
Vmpp (mV)	532.02	383.44	413.56
Impp (mA/m^2)	116.48	229.59	403.03
Rmpp (Ω)	1186.31	435.73	266.81
FF (%)	36.92	36.56	31.84

External loads with resistances within a tolerance limit of ± 10% compared to the actual estimated resistance from the MPP (R_{mpp}) (Table 2) were connected to the respective MFCs. In this case, R1, R0.5 and R0.1 of 1200 Ω, 470 Ω and 270 Ω, respectively, were the closest available resistance in the lab during the study. Figure 4 shows the performance trend of the MFC under these RTELs.

When the external loads were connected, the data logger was reset to take measurements every 10 min as against the initial setting of 1 h. This was necessary to study the short-term and long-term effect of the external loads on the performance of the MFC. Initially (after 10 min) the current density was highest (618.9 mA/m^2) with the 270 Ω resistor and least (147.1 mA/m^2) with the 1.2 kΩ resistor. As presented in Fig. 4a, after 1 h of the MFCs operation under loading, the current decay was 13, 65 and 72% for 1.2 kΩ, 470 Ω, and 270 Ω, respectively. This trend was almost constant with the 1200 and 270 Ω resistors whereas a growth

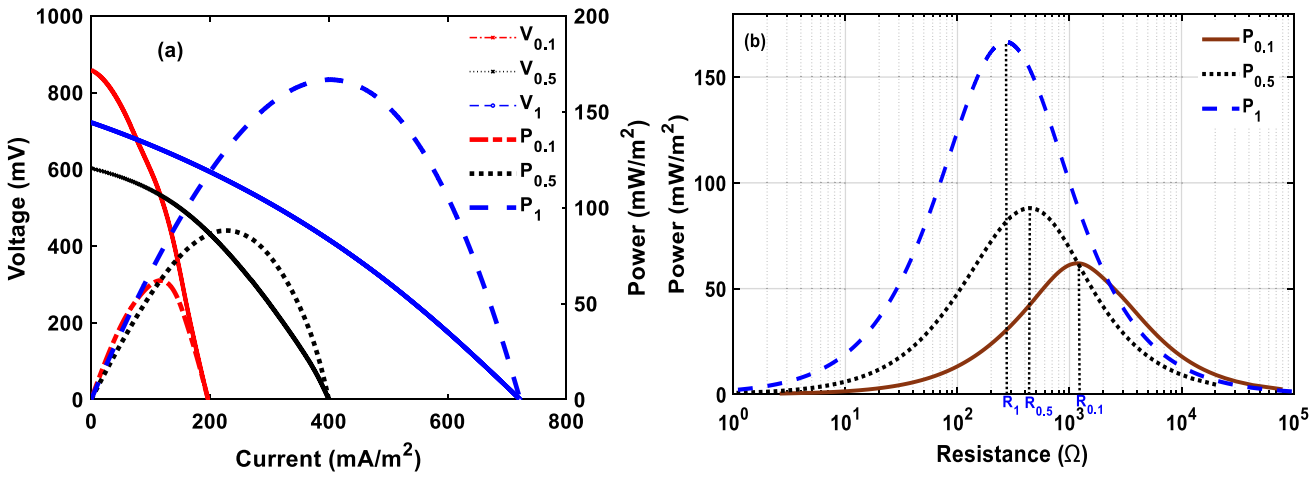

Fig. 3 Performance curve at different PSR during the steady OCV of the MFCs: **a** polarization and power density vs current density, **b** power density vs resistance (the resistance axis is on logarithmic scale for better representation)

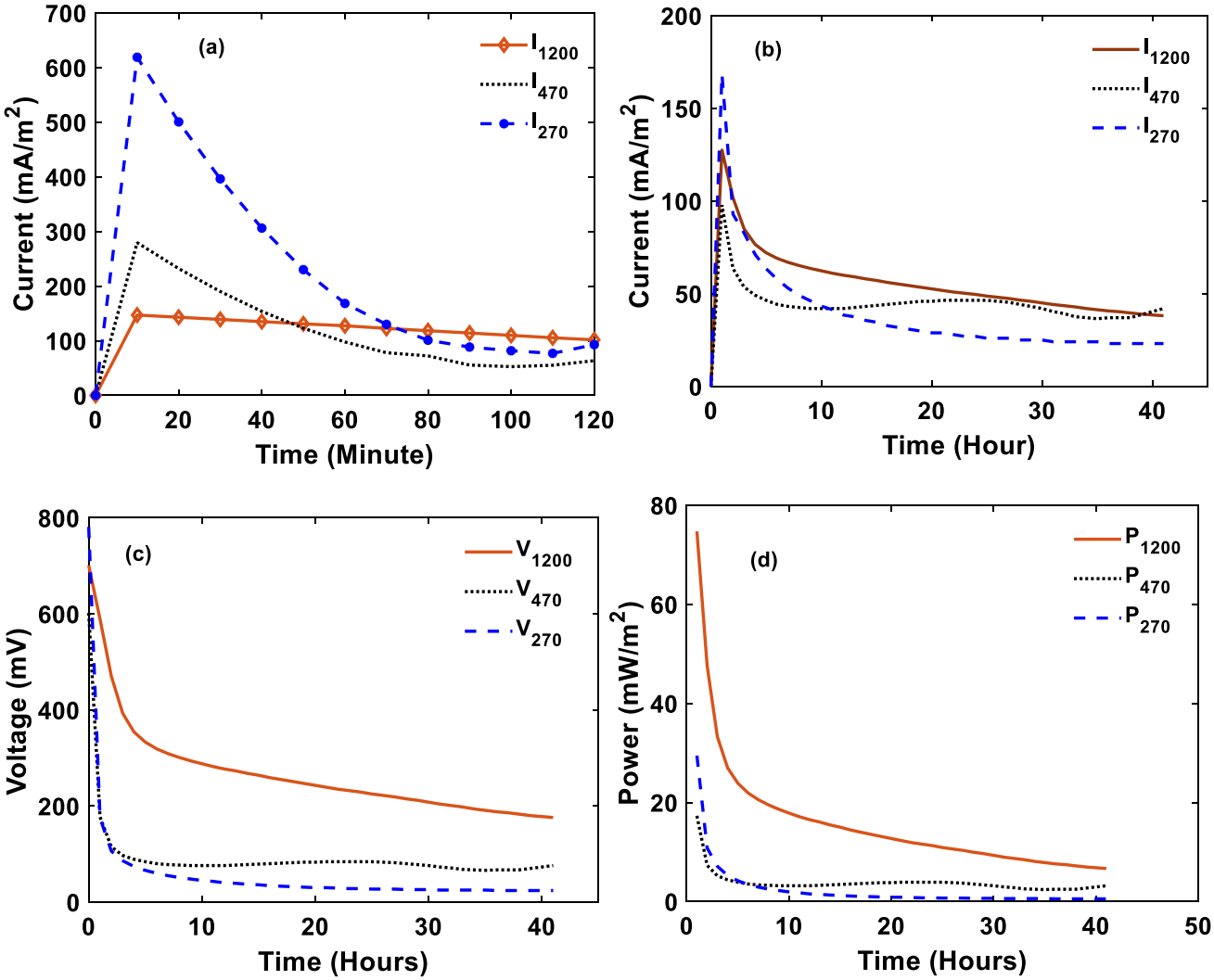

Fig. 4 MFC performance under RTEL during the steady phase in **a** the first two hours, **b**, **c**, **d** over forty hours of operation

in current was observed with the 470 Ω load between the 10th and 25th hour of operation. The least current decay observed with 1200 Ω indicated that the performance was more stable at this external load, whereas the large decay in current at 270 Ω showed that excess current was drawn from the MFC probably higher than the metabolic activities of the EAB could support. This led to the poor performance of the MFC at the smaller resistances over an extended period of operation. As expected, a higher voltage was measured with the highest resistor (Fig. 3c resulting in the long-term better performance of the MFC, in terms of power density (Fig. 4d).

Effects of PSR and RTEL on the performance of MFCs in logarithmic growth phase

There are four distinct phases in the bacterial growth cycle which are usually observed in the voltage development of the MFC. The lag phase represents the phase where no or little observable increase in voltage is observed because bacteria are only metabolically active, but no cell division occurs. At the logarithmic or exponential phase, a rapid increase in voltage is usually observed due to exponential proliferation of the electroactive microbes because of active cells division. There is also the stationary phase when the voltage reaches a plateau and the death phase which is directly opposite the exponential phase (Simeon et al. 2022b). Since the activities of the EAB are highest at the logarithmic phase, it was necessary to evaluate the influence of PSR at this phase. To achieve this, a new experiment was set up, but the MPP parameters were determined during the exponential increase in OCV (Fig. 5).

The power and polarization curves are presented in Fig. 6. The performance indices at the logarithmic phase are shown in Table 3. Like the observation at the stationary phase, MFCs evaluated at higher PSRs produced higher power and

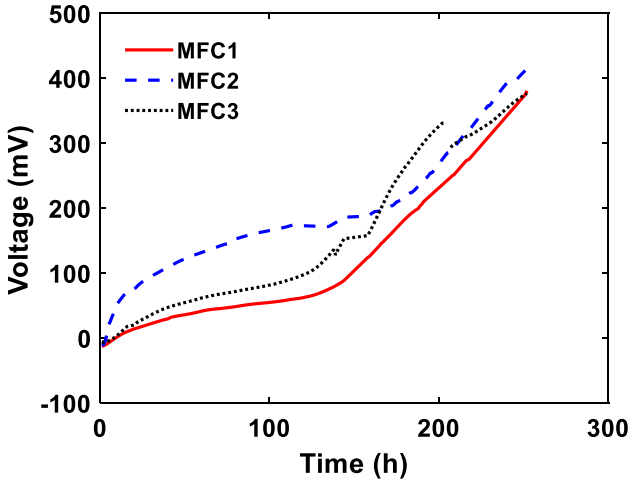

Fig. 5 OCV of MFCs during the logarithmic growth phase before polarization. The lost data with MFC 3 was due to contact problem of the MFC with the terminal board of the data logger

lower resistance. This shows that for this MFC configuration, the power measured using LSV depends on the PSR, irrespective of the phase at which the MFCs are polarized.

Apart from the OCV and the fill factor, all performance indices show a significant difference for the different PSRs. The fill factor was least affected, indicating that the theoretical efficiency of the MFC remains constant regardless of the PSR. The power measured at the MPP, including both P_T and P_{max}, exhibited a positive correlation with the PSR, following a second-degree polynomial relationship (Fig. S2). Conversely, an inverse relationship was observed between power and resistance. It is worth noting that the R_{mpp}s in the stationary phase were all comparable to those in the exponential phase, with a percentage difference of 3.1, 60.1 and 11.6% in the order of increasing PSR, respectively. The biggest difference occurred with the 0.5 PSR.

To evaluate the effects of the RTELs on the performance of the MFC in the logarithmic phase, RTELs of 1200 Ω, 690 Ω and 290 Ω were connected to the MFC polarized at 0.1, 0.5 and 1 mV/s, respectively. The resistors were selected within the tolerance limit of ± 10% of the R_{mpp}. Figure 7 shows the power trends in terms of voltage, current and absolute power of the MFCs with these RTELs.

The performance profiles of the MFCs, presented in Fig. 7, show that after an initial drop in performance, all MFCs gradually increased and reached a steady state before substrate depletion. As expected, the MFC connected to a 1.2 kΩ resistor exhibited higher voltages due to the higher resistor value. However, the MFCs connected to the lower resistive loads did not produce higher currents as anticipated. The growth pattern also indicated that the metabolic activities of the EAB were more favorable at the

Table 3 Performance indices at exponential phase

Parameters	PSR0.1	PSR0.5	PSR1
I_s (mA)	0.358	0.601	1.32
E_{oc} (mV)	381	414	377
P_T (mW)	0.14	0.25	0.5
P_{max} (mW)	0.06	0.11	0.19
V_{mpp} (mV)	269.04	272.12	237.31
I_{mpp} (mA)	0.22	0.39	0.797
R_{mpp} (Ω)	1222.91	697.74	297.75
FF (%)	42.86	44	38

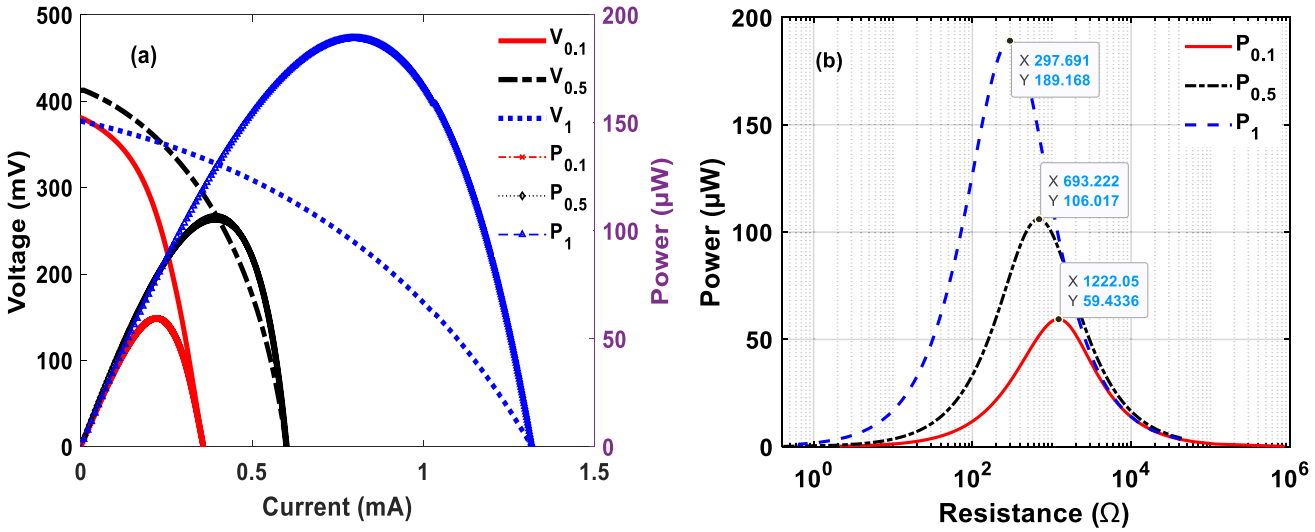

Fig. 6 Performance curves at different PSRs during the logarithmic phase of the MFCs

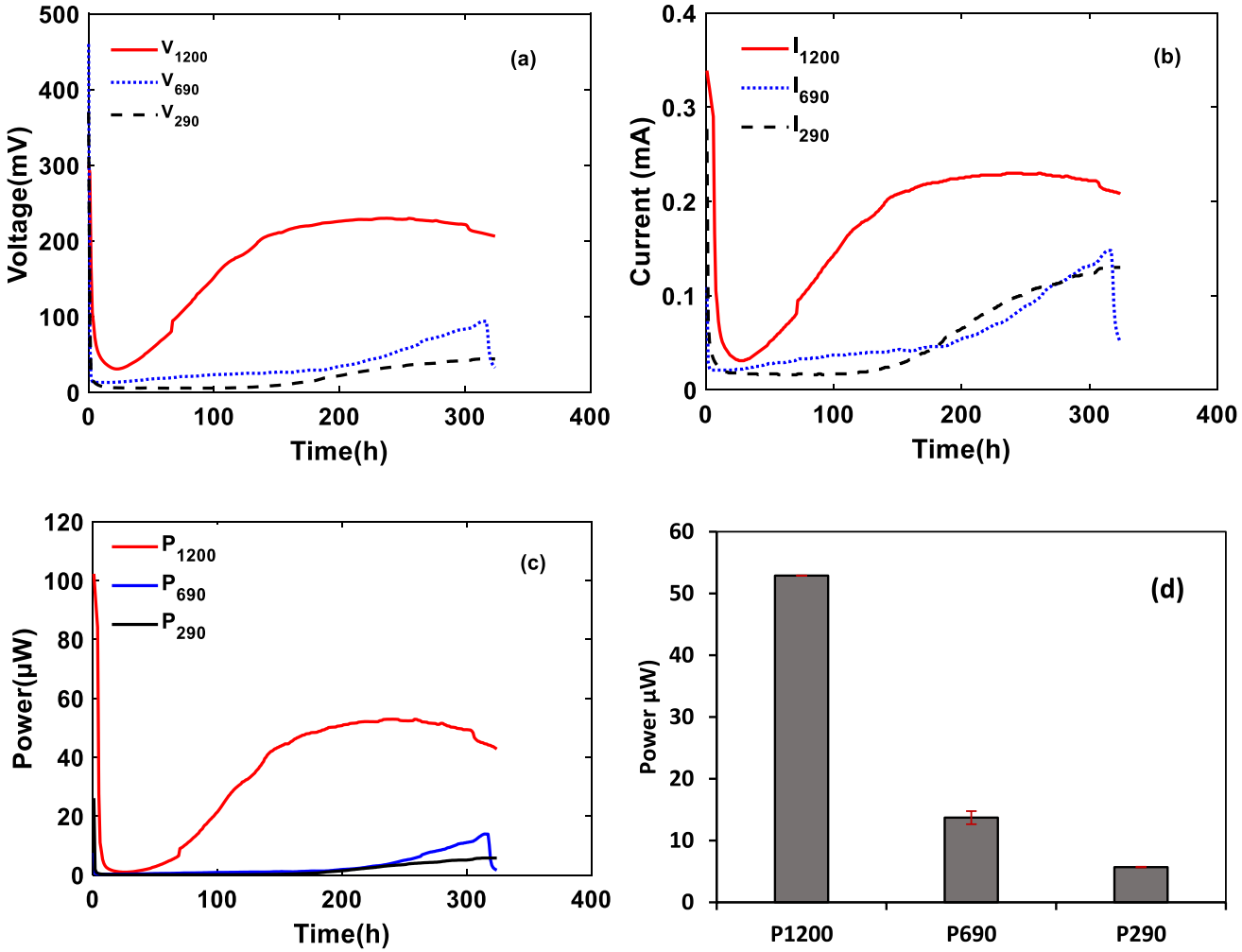

Fig. 7 MFC performance under RTEL **a**, **b**, **c** during the exponential phase, **d** average stable power achieved at the different RTELs

R_{mpp} determined at 0.1 mV/s. This assertion is supported by the establishment of the phases of the normal bacterial growth cycle with the 1.2 kΩ RTEL, which was not observed with the other RTELs. Interestingly, the average steady power (Fig. 7d) obtained with the 1.2 kΩ RTEL is very close to the predicted value at 0.1 mV/s (Table 3). These performance profiles suggest that the choice of the appropriate RTEL is critical to the development and performance efficiency of MFCs. This agrees with findings by Koók et al., who reported that the electrical load significantly affects the efficiency of MFCs, including biofilm formation and cell metabolism (Koók et al. 2021). Phases of exponential increase in performance were observed in Fig. 7a–c. This was expected, as the external loads were connected when microbial metabolism was at its peak (indicated by the exponential voltage growth before the LSVs were performed). The LSV tests are valuable for determining the characteristics of the functioning soil MFCs, in this case. They suggested that MFC performance could be maximized by connecting the appropriate external loads to the MFCs immediately after the start-up phase and that performing LSV at a low scan rate can help in selecting the correct resistor for operating the MFC. Currently, external loads for operating MFCs are often selected arbitrarily, which is not sufficiently scientific.

The lack of operational stability at the lower resistance further elucidates the criticality of the specific roles of external loads in capturing maximum power from microbes using MFC as was previously reported (Koók et al. 2020). In this case, a PSR of 0.1 mV/s more accurately estimated the internal resistance of the soil MFC used in this study. In addition to operational stability, operating the MFC at the RTEL close to the internal resistance ensured maximum power extraction from the MFC according to the principle of maximum power transfer.

Estimating the time to obtain equivalent performance from RTEL and LSV at different PSRs

Figure 8 shows the point of intersection of the power measured from MPP at the different PSRs and the power produced at the estimated RTELs. It took about 85 min for the actual power to match the predicted power at 0.1 mV/s, while it took 30 min for the power at 1 mV/s to match. This could be an indication of how long resistors should be connected when the polarization sweep is determined manually with a variable resistor or with different resistors technically selected for the system under study.

Finding RTEL for the best performance of the single chamber soil MFC

In addition to determining the best PSR for evaluating the long-term performance of the MFC with capacitive electrodes used in this study, different external loads with resistance range of 200–2000 Ω were arbitrarily selected. The performance trends of the MFC when the external loads were connected at the steady state are shown in Fig. 9.

A single MFC that had performed consistently (steady-state performance) for at least three months was used to study the effect of RTEL. It was necessary to avoid experimental bias due to inherent differences between different MFCs. The MFC was discharged (starting with the highest resistance) for at least 12 h under constant load discharge (EC-lab, V11.32). After each discharge cycle, the MFC was allowed to regain its steady-state performance before the next discharge cycle. Discharging the MFC across each RTEL for at least 12 h (Fig. 9), the performance increased from 200 to 1 kΩ. Further increasing the R_{ext} did not further improve the performance. This showed that the soil MFC configuration employed in this study has an optimum performance around 1 kΩ RTEL, which is within 17% of the

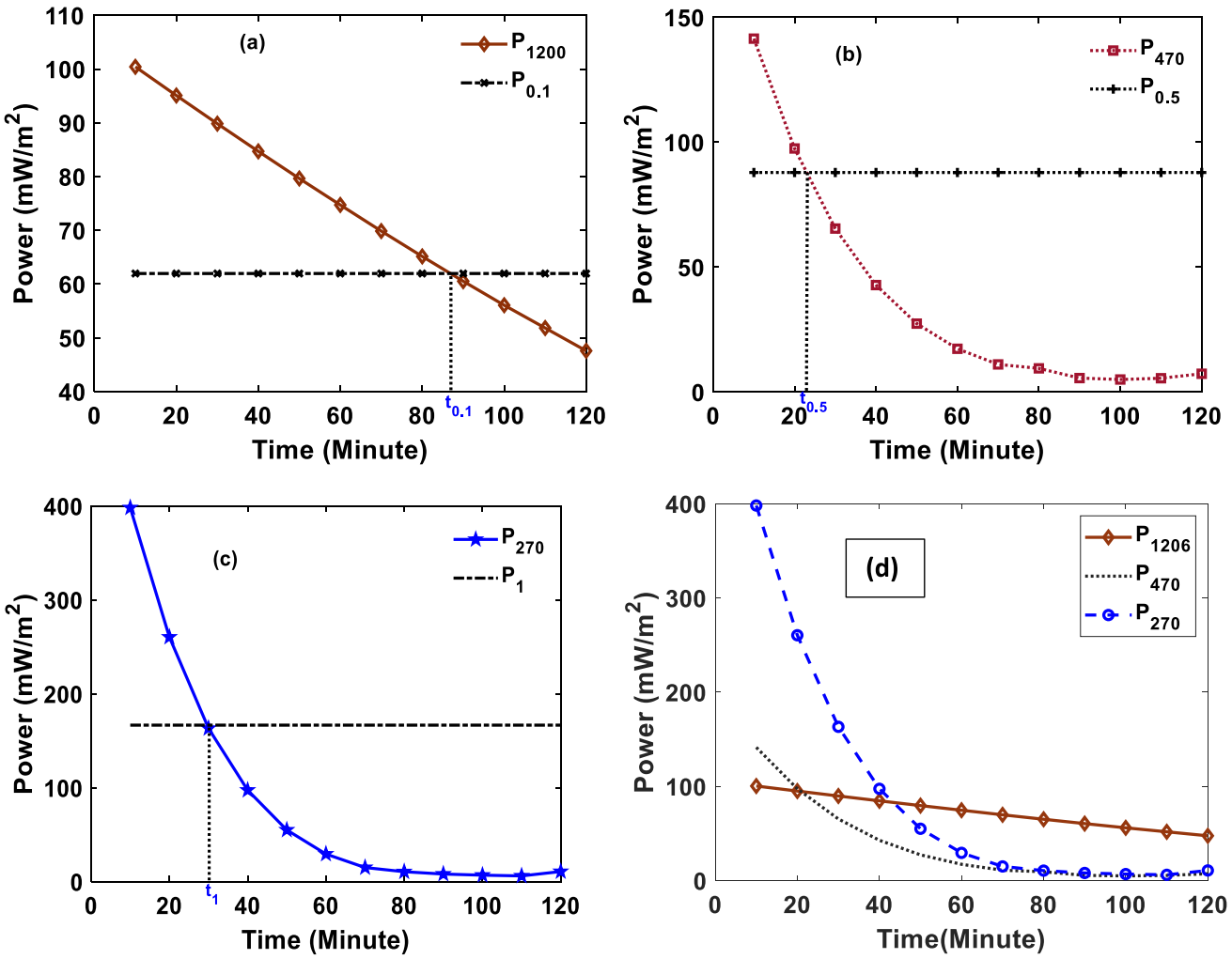

Fig. 8 Time of intersection of the Pmax obtained from different PSRs and the performance with the equivalent RTELs determined from the MPPs (**a**–**c**); comparing the performance of the MFCs with 1200, 470 and 270 Ω RTELs

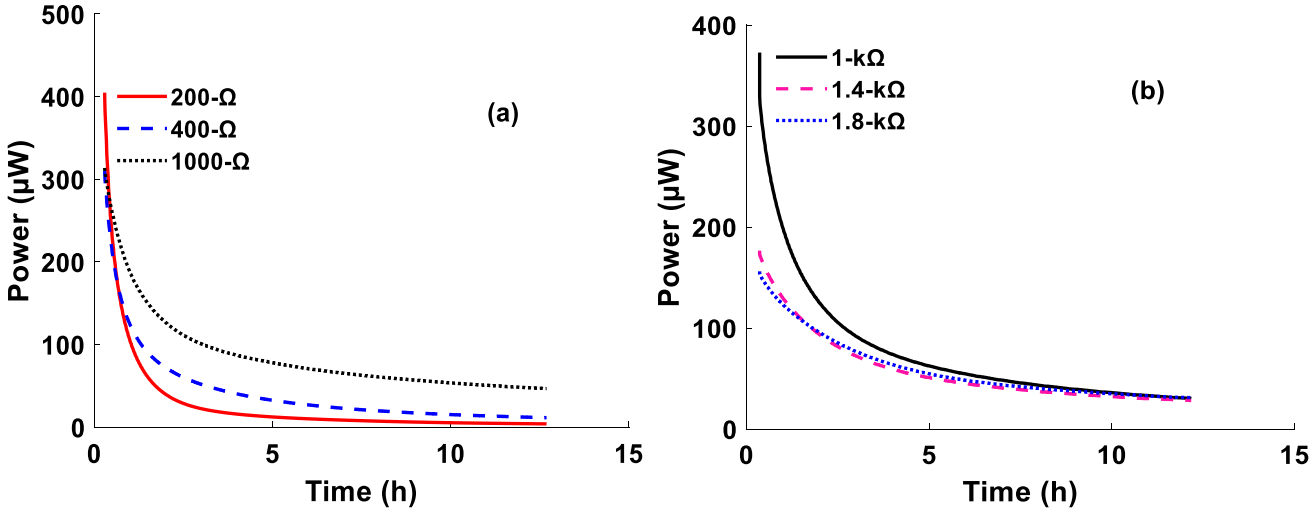

Fig. 9 Influence of external resistance on SMFC's performance

lower tolerance limit of the optimum load determined from the LSV at a PSR of 0.1 mV/s.

Conclusion

Linear sweep voltammetry remains a useful tool for evaluating and comparing the maximum power point of MFCs. For the three potential scan rates (PSR) tested in this study, a PSR of 0.1 mV/s more accurately reflected the true and applicable estimate of the long-term performance of the soil MFC when the external loads were connected at different operating phases. With the correct PSR, an external resistance can be obtained from the MPP to extract maximum and sustained power from the MFC. The power profiles at different external loads in this study support the claim that external loads not only have a large impact on the efficiency of the MFC, but also on biofilm formation and cell metabolism within the MFC. Performing the polarization sweep manually with technically selected resistors may require a longer period than the currently used 10–20 min if the results are to be comparable to the power measured with a potentiostat at a PSR of 0.1 mV/s. Furthermore, based on the result obtained from this study, it can be inferred that: (a) maximum power can be achieved from LSV data with values that closely match those obtained using the optimal RTEL, (b) with an RTEL of 1200 Ω, determined from the polarization sweep at 0.1 mV/s, the power output was maximized and maintained over an extended operating period, (c) for the MFC configuration used in this study, a PSR of 0.1 mV/s provided an external load at which the MFC performance was both optimal and sustainable. Further studies are needed to determine the best PSR value for different MFC configurations with different electrodes and substrates. The development of a universally accepted PSR and optimum RTEL values for different MFC systems would facilitate and standardize the comparison of the electrochemical performance of MFCs in different studies. Finally, the findings from this study suggest that the optimal PSR and RTEL for long-term MFC performance differ from commonly used rates and values, highlighting the need to revise standard testing protocols for different MFCs configurations. Standardizing protocols with optimal PSRs and RTEL will improve the comparability of results across studies, establish reliable performance benchmarks, and provide better guidance for practical applications of MFCs. This will enhance the consistency and relevance of MFC performance evaluations, advancing the field.

Supplementary Information The online version contains supplementary material available at https://doi.org/10.1007/s13762-024-05989-8.

Author contributions Conceptualization: IMS; Design. Material preparation, data collection and analysis: IMS. Original draft preparation: IMS, RF, AG. Review and editing: IMS, RF, AG; Project administration and supervision: RF. All authors commented on previous versions of the manuscript. All authors read and approved the final manuscript.

Funding Open Access funding enabled and organized by Projekt DEAL. This research did not receive any specific grant from funding agencies in the public, commercial, or not-for-profit sectors.

Declarations

Conflict of interest The authors declared that they have no conflict of interest.

Ethical approval This article does not contain any studies with human participants or animals performed by any of the authors.

Consent to participate All the authors are informed and agree to this study.

Consent for publication All the authors agree to publication in this journal.

References

Aghababaie M, Farhadian M, Jeihanipour A, Biria D (2015) Effective factors on the performance of microbial fuel cells in wastewater treatment–a review. Environmental Technology Reviews. https://doi.org/10.1080/09593330.2015.1077896

Ameen M, Zafar M, Ahmad M, Sultana S, Makhkamov T, Yuldashev A, Mamarakhimov O, Nasirov M, Kilic O, Ozdemir FA, Gafforov Y (2024) Prospects of bioenergy development in future. Encyclopedia of Renewable Energy, Sustainability and the Environment. Elsevier, pp 497–508. https://doi.org/10.1016/B978-0-323-93940-9.00024-4

Anika OC, Nnabuife SG, Bello A, Okoroafor ER, Kuang B, Villa R (2022) Prospects of low and zero-carbon renewable fuels in 1.5-degree net zero emission actualisation by 2050: a critical review. Carbon Capture Sci Technol 5:100072

Golzarian M, Ghiasvand M, Shokri S et al (2024) Performance evaluation of a dual-chamber plant microbial fuel cell developed for electricity generation and wastewater treatment. Int J Environ Sci Technol. https://doi.org/10.1007/s13762-023-05415-5

Kim Y, Hatzell MC, Hutchinson AJ, Logan BE (2011) Capturing power at higher voltages from arrays of microbial fuel cells without voltage reversal. Energy Environ Sci 4:4662–4667. https://doi.org/10.1039/c1ee02451e

Koók L, Nemestóthy N, Bélafi-Bakó K, Bakonyi P (2020) Investigating the specific role of external load on the performance versus stability trade-off in microbial fuel cells. Bioresour Technol. https://doi.org/10.1016/j.biortech.2020.123313

Koók L, Nemestóthy N, Bélafi-Bakó K, Bakonyi P (2021) The influential role of external electrical load in microbial fuel cells and related improvement strategies: a review. Bioelectrochemistry. https://doi.org/10.1016/j.bioelechem.2021.107749

Lepage G, Perrier G, Merlin G, Aryal N, Dominguez-Benetton X (2014) Multifactorial evaluation of the electrochemical response of a microbial fuel cell. RSC Adv 4(45):23815–23825. https://doi.org/10.1039/C4RA03879G

Li Q, Wang Y, An C, Jia H, Wang J (2024) Exploring novel approaches to enhance start-up process in microbial fuel cell: a comprehensive review. J Water Process Eng 63:105425. https://doi.org/10.1016/j.jwpe.2024.105425

Littfinski T, Nettmann E, Gehring T, Krimmler S, Heinrichmeier J, Murnleitner E, Lübken M, Pant D, Wichern M (2021) A comparative study of different electrochemical methods to determine cell internal parameters of microbial fuel cells. J Power Sour. https://doi.org/10.1016/j.jpowsour.2021.2297075

Logan BE, Hamelers B, Rozendal R, Schröder U, Keller J, Freguia S et al (2006) Microbial fuel cells: methodology and technology. Environ Sci Technol 40(17):5181–5192. https://doi.org/10.1021/es0605016

Miao G, Chunfei W, Stephen C, Xi Y, Tom V, Astley H, Pete S, Nilay S (2023) Advances in biorenewables-resource-waste systems and modelling. Carbon Capture Sci Technol 9:100142. https://doi.org/10.1016/j.ccst.2023.100142

Nam T, Son S, Kim E, Tran HVH, Koo B, Chai H, Kim J, Pandit S, Gurung A, Oh SE, Kim EJ, Choi Y, Jung SP (2018) Improved structures of stainless-steel current collector increase power generation of microbial fuel cells by decreasing cathodic charge transfer impedance. Environ Eng Res 23:383–389. https://doi.org/10.4491/eer.2017.171

Nawaz A, Hafeez A, Abbas SZ, Haq ul I, Mukhtar H, Rafatullah M (2020) A state of the art review on electron transfer mechanisms, characteristics, applications and recent advancements in microbial fuel cells technology. Green Chem Lett Rev. https://doi.org/10.1080/17518253.2020.1854871

Pandit S, Das D (2018) Principles of microbial fuel cell for the power generation. In: Das D (ed) microbial fuel cell. Springer International Publishing, Cham, pp 21–41. https://doi.org/10.1007/978-3-319-66793-5_2

Peng X, Yu H, Yu H, Wang X (2013) Lack of anodic capacitance causes power overshoot in microbial fuel cells. Bioresour Technol 138:353–358. https://doi.org/10.1016/j.biortech.2013.03.187

Poli F, Seri J, Santoro C, Soavi F (2020) Boosting microbial fuel cell performance by combining with an external supercapacitor: an electrochemical study. ChemElectroChem 7:893–903. https://doi.org/10.1002/celc.201901876

Saadi M, Pézard J, Haddour N, Erouel M, Vogel TM, Khirouni K (2020) Stainless steel coated with carbon nanofiber/PDMS composite as anodes in microbial fuel cells. Mater Res Express. https://doi.org/10.1088/2053-1591/ab6c99

Simeon MI (2023) Optimization of Soil Microbial Fuel Cell for Sustainable Bioelectricity Generation and Bioremediation. Verlag Dr, Koster, Berlin

Simeon M, Freitag R (2022) Influence of electrode spacing and fed-batch operation on the maximum performance trend of a soil microbial fuel cell. Int J Hydrogen Energy. https://doi.org/10.1016/j.ijhydene.2021.11.110

Simeon MI, Raji AO (2016) Experimental utilization of urine to recharge soil microbial fuel cell for constant power generation. Res J Eng Environ Sci 1:129–135

Simeon MI, Herkendell K, Pant D, Freitag R (2022a) Electrochemical evaluation of different polymer binders for the production of carbon-modified stainless-steel electrodes for sustainable power generation using a soil microbial fuel cell. Chem Eng J Adv. https://doi.org/10.1016/j.ceja.2022.100246

Simeon IM, Weig A, Freitag R (2022b) Optimization of soil microbial fuel cell for sustainable bio-electricity production: combined effects of electrode material, electrode spacing, and substrate feeding frequency on power generation and microbial community diversity. Biotechnol Biofuels Bioprod. https://doi.org/10.1186/s13068-022-02224-9

Simeon M, Otache MY, Ewemoje TA, Raji AO (2019) Application of urine as fuel in a soil-based membrane-less single chamber microbial fuel cell. Agricultural Engineering International: CIGR Journal

Simeon MI, Imoize AL, Freitag R (2021) Comparative evaluation of the performance of a capacitive and a non-capacitive microbial fuel cell. In: 18th IEEE International Multi-Conference on Systems, Signals and Devices, SSD. https://doi.org/10.1109/SSD52085.2021.9429481

Vinoth Kannan SR, Ganesan NG, Samal S, Dey P, Manjare SD, Rangarajan V (2023) Mitigation of environment crisis: conversion of organic plant waste to valuable products. Valorization of Wastes

for Sustainable Development. Elsevier, pp 33–65. https://doi.org/10.1016/B978-0-323-95417-4.00002-0

Walter XA, Gajda I, Forbes S, Winfield J, Greenman J, Ieropoulos I (2016) Scaling-up of a novel, simplified MFC stack based on a self-stratifying urine column. Biotechnol Biofuels. https://doi.org/10.1186/s13068-016-0504-3

Walter XA, Santoro C, Greenman J, Ieropoulos I (2019) Self-stratifying microbial fuel cell: The importance of the cathode electrode immersion height. Int J Hydrogen Energy. https://doi.org/10.1016/j.ijhydene.2018.07.033

Wang Z, Lee T, Lim B, Choi C, Park J (2014) Microbial community structures differentiated in a single-chamber air-cathode microbial fuel cell fueled with rice straw hydrolysate. Biotechnol Biofuels. https://doi.org/10.1186/1754-6834-7-9

Watson VJ, Logan BE (2011) Analysis of polarization methods for elimination of power overshoot in microbial fuel cells. Electrochem Commun 13:54–56. https://doi.org/10.1016/j.elecom.2010.11.011

Zhao F, Slade RCT, Varcoe JR (2009) Techniques for the study and development of microbial fuel cells: an electrochemical perspective. Chem Soc Rev 38:1926–1939